

1 **Pliocene crustal shortening on the Tyrrhenian side of the northern Apennines: evidence**  
2 **from the Gavorrano antiform (southern Tuscany, Italy)**

3

4 Giovanni Musumeci<sup>a</sup>, Francesco Mazzarini<sup>b</sup> & Marco Barsella<sup>a</sup>

5 a: Dipartimento di Scienze della Terra, Università di Pisa, Via S.Maria, 53, Pisa 56126, Italy

6 b: Istituto Nazionale di Geofisica e Vulcanologia, Sezione di Pisa, Pisa, Italy.

7

8

9

10 Corresponding author:

11 Giovanni Musumeci

12 Dipartimento di Scienze della Terra, Università di Pisa, Via S.Maria, 53, Pisa 56126, Italy,

13 Fax: +39 050 2215800 – email: gm@dst.unipi.it

14

15 Words: 6891

16 References: 47

17 Figures: 8

18 Table: 1

19

20 Abbreviated title: Inner northern Apennines Pliocene shortening

21

22

23 **Abstract**

24 The northern Tyrrhenian Sea and the inner northern Apennines are classically regarded as a  
25 late Miocene-Pleistocene back-arc system developed as a consequence of slab roll-back along  
26 active subduction zones. We present new geological and structural data on the Gavorrano  
27 antiform, a key sector of the inner northern Apennines. Lying close to the northern Tyrrhenian  
28 Sea, it provides clear evidence of Pliocene shortening deformation and magma emplacement.  
29 The orientation of  $\sigma_1$  (N50°E - N80°E) derived by fault slip data inversion is consistent with a  
30 general ENE –WSW shortening direction. Furthermore, this ENE-trending orientation of  $\sigma_1$  is  
31 compatible with the compressive deformation recorded in coeval sedimentary basins. On this  
32 basis we suggest that the inner northern Apennines were affected by crustal shortening during  
33 the Pliocene. This scenario matches well geophysical data suggesting that since the Late  
34 Messinian (6 – 5 Ma) subduction rollback and back-arc extension strongly decreased in the  
35 northern Tyrrhenian Sea, while they continued as active processes in the southern Tyrrhenian  
36 Sea.

37

38

39

40 *Key words: crustal shortening, Alpine tectonics, Pliocene, northern Apennines*

41

42 The Mediterranean region is an area of Cenozoic continental convergence in which Alpine  
43 thrust belts surround back-arc basins developed as a consequence of slab roll-back along  
44 active subduction zones. The Balearic, Alboran and southern Tyrrhenian basins are the best  
45 examples of back-arc systems in hinterland portions of Alpine chains, in which extension and  
46 growth of new oceanic crust were coeval with shortening at the front of the chain (Faccenna  
47 *et al.*, 2004, Platt 2007). The Tyrrhenian Sea at the rear of the Apennine chain opened because  
48 of the eastward roll-back of the Adria Plate, which had been subducting westward beneath the  
49 European margin (Malinverno & Ryan 1986; Royden *et al.* 1987; Rosenbaum & Lister 2004).  
50 The opening of the Tyrrhenian Sea started in the Late Miocene and culminated with seafloor  
51 spreading in the south Tyrrhenian during the Pliocene – Pleistocene (Nicolosi *et al.*, 2006;  
52 Rosenbaum & Lister 2004).

53 In this scenario, the northern Tyrrhenian Sea basin and the inner northern Apennines  
54 are classically regarded as a late Miocene-Pleistocene back-arc system characterised by  
55 crustal extension and acidic magmatism coeval with shortening at the front of the chain  
56 (Carmignani *et al.*, 1994; Jolivet *et al.*, 1998). In the northern Tyrrhenian Sea, the occurrence  
57 of asthenospheric mantle at a depth of 25 km testifies to lithosphere thinning, which is  
58 ascribed to slab roll back (Della Vedova *et al.* 1991). Asthenospheric upwelling beneath the  
59 Late Miocene chain produced a regional-scale positive thermal anomaly (Baldi *et al.* 1994)  
60 which triggered the development of Late Miocene - Quaternary magmatism (Fig. 1),  
61 represented by intrusive and volcanic rocks distributed over a wide area between the northern  
62 Tyrrhenian Sea and the inner northern Apennines (Innocenti *et al.* 1992).

63 According to Carmignani *et al.* (1994) and Decandia *et al.* (1998), proof of Late  
64 Miocene –Pliocene crustal extension in the inner northern Apennines is provided by low- and  
65 high-angle normal faults that controlled the development of sedimentary basins (Carmignani  
66 *et al.* 1994; Keller *et al.* 1994; Brogi *et al.* 2003) and the emplacement of Neogene intrusions

67 (Acocella & Rossetti 2002), whose emplacement ages indicate an eastward migration of  
68 magmatism from the Tyrrhenian Sea (6–7 Ma) inland (4–0.5 Ma).

69 In contrast, there are several examples of compressive structures (folds and faults) in  
70 Upper Miocene – Pleistocene sedimentary basins (e.g. Meletti *et al.* 1995; Boccaletti *et al.*  
71 1997; Boccaletti & Sani 1998). These structures have been interpreted as evidence that crustal  
72 shortening was still active in the inner northern Apennines during the opening of the northern  
73 Tyrrhenian Sea. Furthermore, recent seismic anisotropy data question the role of subduction  
74 in the northern Tyrrhenian sea, indicating the presence of true back-arc basins only in the  
75 southern Tyrrhenian sea (Plomerova *et al.*, 2006; Levin *et al.*, 2007; Salimbeni *et al.*, 2007).

76 This paper aims to unravel the nature of Pliocene tectonics in the inner northern  
77 Apennines. New data and interpretations arise from the analysis of the Gavorrano antiform  
78 (Fig. 2) near the Tyrrhenian coast of southern Tuscany. In this structure, a complete sequence  
79 of the nappe pile resulting from Miocene deformation is well exposed together with Pliocene  
80 intrusive rocks and Upper Miocene – Upper Pliocene - Pleistocene sedimentary deposits. By  
81 combining new data with published findings, we develop a coherent framework for Pliocene  
82 shortening in the northern Apennines.

83

#### 84 **Geological setting of northern Apennines in southern Tuscany**

85 The northern Apennines (Fig. 1), a fold-thrust belt of the Alpine orogen, resulted from the  
86 Cenozoic continental collision between the European margin (Corsica-Sardinia microplate)  
87 and the Adria Plate after closure of the Tethyan Ocean (Boccaletti *et al.* 1971). In the inner  
88 northern Apennines (Tuscan domain), the fold belt consists of a nappe stack of Meso-  
89 Cenozoic sedimentary and metamorphic tectonic units derived from an oceanic domain  
90 (Ligurian Units) and the Adria continental margin (Tuscan Nappe and Tuscan Metamorphic  
91 Complex). The nappe stack was produced by Late Oligocene – Early-Middle Miocene

92 deformation, during which the tectonic units experienced polyphase deformation with the  
93 development of eastward-facing fold and thrust structures.

94 Southern Tuscany is a portion of the inner northern Apennines located south of Monti  
95 Pisani and extending southward to the Monte Argentario promontory; the northern Tyrrhenian  
96 Sea borders the area to the west (Fig. 1). In this region the Apennine nappe stack consists of  
97 two structural and metamorphic levels (Fig. 1). The upper level is made up of sedimentary or  
98 very low-grade metamorphic thrust sheets belonging to Ligurian Units and the Tuscan Nappe.  
99 The lower level is the Tuscan Metamorphic Complex, which is represented by low-grade  
100 metamorphic rocks derived from reworked Paleozoic basement and a Permian–Triassic  
101 sedimentary sequence (Musumeci *et al.* 2002). The Tuscan Metamorphic Complex, which  
102 experienced alpine deformation under Barrovian (MP/MT) metamorphic conditions  
103 (Franceschelli *et al.* 1986), crops out along the Mid-Tuscan Ridge (Fig. 1) but more widely  
104 occurs as units buried at depths below 2 km in the Larderello geothermal field, where it has  
105 been penetrated by deep geothermal boreholes. The earlier nappe stacking was followed in the  
106 Middle Miocene (Langhian – Serravallian) by renewed deformation, which led to the tectonic  
107 omission of large part of the Tuscan Nappe stratigraphic sequence and the anomalous  
108 superpositioning of Ligurian Units directly onto the basal (Triassic) formation of the Tuscan  
109 Nappe or, in some instances, directly onto the metamorphic rocks of the Tuscan Metamorphic  
110 Complex. This structural setting (the so-called “Serie ridotta”; Giannini *et al.* 1971; Bertini *et*  
111 *al.* 1994) has been interpreted as the result of either Middle Miocene extension of the chain  
112 (Carmignani *et al.* 1994; Jolivet *et al.* 1998) or crustal shortening with the development of an  
113 out-of-sequence thrust at the base of the Ligurian Units (Finetti *et al.* 2001). At the scale of  
114 the whole northern Apennines, Middle Miocene deformation was possibly responsible for  
115 formation of the Alpi Apuane core complex (Carmignani & Kligfield, 1990). Alternatively,

116 the Alpi Apuane structure was produced by out-of sequence thrusts (Storti, 1995; Boccaletti  
117 & Sani, 1998).

118         Whatever the process, as a result of Middle Miocene deformation the sedimentary  
119 sequence of the Tuscan Nappe is often largely omitted in southern Tuscany; it is almost  
120 completely preserved in only a few areas. These correspond to the cores of km-scale N- and  
121 NNW-trending antiforms that are best exemplified by the Campiglia and Gavorrano antiforms  
122 along the Tyrrhenian coast and by the Cornate – Travale antiforms in the Larderello  
123 geothermal field (Fig. 1). The tectonic units are covered by Neogene (Late Miocene –  
124 Pleistocene) sediments that were deposited within hinterland sedimentary basins filled by  
125 continental (conglomerates) and shallow marine (evaporites, limestones) deposits.

126         In the Pliocene, intrusive and volcanic rocks (Innocenti *et al.* 1992) were emplaced in  
127 the nappe stack. The latter are rhyolites and trachytes, which are mainly exposed on the Mt.  
128 Amiata volcano. Intrusive rocks crop out as small bodies in the Campiglia and Gavorrano  
129 areas, or as shallow (3 – 5 km) buried intrusions in the Larderello geothermal field (Bertini *et*  
130 *al.* 2006; Dini *et al.* 2004; Gianelli *et al.* 1997). Granite emplacement within the Tuscan  
131 Metamorphic Complex and Tuscan Nappe sequences led to the development of LP/HT  
132 contact aureoles with hydrothermal and ore deposits (Carella *et al.* 2000; Musumeci *et al.*  
133 2002). The age of magmatism in southern Tuscany is bracketed between 4.4 Ma (Castel di  
134 Pietra and Gavorrano Granite; Serri *et al.* 1993) and 02–0.3 Ma (Mt. Amiata trachytic dacite;  
135 Savelli 2000).

136

### 137 **Geological setting of the Gavorrano structure**

138 The Gavorrano antiform lies south of the Larderello geothermal field and close to the  
139 Tyrrhenian coast (Fig. 1). It is a NNW-trending antiform in which a complete sequence of

140 tectonic units (from the Tuscan Metamorphic Complex to the Tuscan Nappe and Ligurian  
141 Unit) as well as Pliocene intrusive rocks crop out (Fig. 2).

142         The lowermost unit (Tuscan Metamorphic Complex) consists of low-grade phyllites  
143 and metasandstones of the Mid-Late Triassic Verrucano Formation. This unit is tectonically  
144 overlain by the Tuscan Nappe (Burgassi *et al.* 1983), a unit representing a complete  
145 sedimentary sequence of Upper Triassic evaporites (Burano Formation) to Upper Oligocene–  
146 Lower Miocene arenaceous flysch (Macigno Formation). The Burano Formation (anhydrites  
147 and dolomites) at the base of the sequence represents the décollement surface along which the  
148 Tuscan Nappe was detached from its substratum and is in tectonic contact with the underlying  
149 Tuscan Metamorphic Complex. A sedimentary sequence with a thickness of nearly 1400 m  
150 lies above the Burano Formation; it consists of Upper Triassic-Jurassic platform and pelagic  
151 carbonate deposits (Calcere e marne a Rhetavicula Formation., Calcere massiccio Formation,  
152 Rosso ammonitico Formation, Calcere selcifero Formation and Marne a Posidonia  
153 Formation). This sequence is followed by Upper Jurassic pelagic siliceous sediments (Diaspri  
154 Formation) and finely laminated limestone (Maiolica Formation). The uppermost portion of  
155 the sequence consists of Cretaceous to Oligocene red-green argillites with intercalated  
156 limestone (Scaglia Formation), followed by Upper Oligocene–Lower Miocene arenaceous  
157 flysch (Macigno Formation). Most of the sedimentary sequence consists of Lower Jurassic  
158 carbonate and Cretaceous to Oligocene pelagic sediments, which maintain constant  
159 thicknesses of nearly 600 m and 500 m, respectively. In contrast, the Jurassic and Cretaceous  
160 pelagic deposits are relatively thin (30 – 100 m) with strong lateral variations. The uppermost  
161 tectonic unit, the Ligurian Unit, consists of Cretaceous to Eocene argillites and calcareous-  
162 marly flysch sequences belonging to the Santa Fiora Unit. They represent the pelagic  
163 sedimentary cover of Jurassic to Cretaceous ophiolitic complexes. The tectonic contact with

164 the underlying Tuscan Nappe corresponds to a metre-sized fault zone with tectonized blackish  
165 argillites, siltites and silicified limestone.

166 The intrusive rocks cropping out in the core of the antiform correspond to the  
167 Gavorrano Granite, which consists of two facies: (i) a dominant porphyritic monzogranite  
168 hosting (ii) decametre- to hectometre-sized tourmaline-bearing leucogranite dikes (Mazzarini  
169 *et al.* 2004). The overall shape of the intrusion corresponds to a NNW-SSE elongated  
170 laccolith parallel to the antiform axis and emplaced along the tectonic contact between the  
171 Tuscan Metamorphic Complex and the Tuscan Nappe. As reported by Mazzarini *et al.* (2004),  
172 the flat base of the intrusion is in contact with the Tuscan Metamorphic Complex, whereas the  
173 roof intrudes the evaporitic décollement level (Burano Formation) at the base of the Tuscan  
174 Nappe, where marble and calc-silicate hornfels represent a hectometre-thick contact aureole  
175 developed in the Upper Triassic-Lower Jurassic carbonate formations.

176 The Gavorrano structure is covered by Neogene continental clastic deposits that crop  
177 out on the northern and south-eastern sides. These deposits comprise an Upper Miocene  
178 conglomerate and Upper Pliocene-Pleistocene conglomerate (Bossio *et al.* 1993). The Upper  
179 Miocene conglomerate consists of clast-supported red conglomerates derived from Ligurian  
180 Units with alternating sand and clay horizons. The Upper Pliocene-Pleistocene conglomerate  
181 is a poorly sorted, matrix-supported polygenic conglomerate composed largely of clasts  
182 derived from Tuscan Nappe Mesozoic formations and the Gavorrano Granite.

183

#### 184 **Structural setting of the antiform**

185 The antiformal shape of the Gavorrano structure is indicated by the opposing dips of  
186 foliations in the Tuscan Nappe formations cropping out on both the western and eastern flanks  
187 (Figs. 2 and 3). The folded foliations are (i) the  $S_0$  sedimentary bedding, (ii) an  $S_1$  foliation  
188 and (iii) a hornfels texture in the contact aureole. The  $S_1$  foliation is well-developed in the



189 pelitic and marly rocks of the Tuscan Nappe formations; it is the axial plane schistosity of  
190 tight to isoclinal recumbent folds that almost completely transposed the  $S_0$  sedimentary  
191 layering. In agreement with Carmignani *et al.* (1994), we interpret these earlier structures as  
192 related to nappe stacking. In the contact aureole, the hornfels texture in marbles and calc-  
193 silicates is characterised by a coarse-grained, equant granoblastic polygonal texture resulting  
194 from the recrystallization of lower Mesozoic carbonate sedimentary bedding.

195 As shown in cross-section, the Gavorrano antiform is a NNW-trending open anticline  
196 dissected by reverse and normal faults (Fig. 3) with a steeply dipping axial plane and a  
197 N160°E-trending fold axis (Fig. 4). On the western flank there are two minor structures of  
198 hectometre wavelength: an open anticline and a syncline (Fig. 2) with axes that plunge gently  
199 to the SE.

#### 200 *F2 fold structures*

201 At the mesoscopic scale, the antiform-related structures are represented by small-scale NNW-  
202 trending folds ( $F_2$ ) with amplitudes of metres to decametres. They occur on both flanks, and  
203 the best exposures are in the hinge zone and in the western flank of the antiform. The  $F_2$  folds  
204 are well expressed in the Diaspri and Maiolica formations cropping out on the western flank  
205 of the antiform (Fig. 2). Here the  $F_2$  folds range from open to tight upright folds of metre to  
206 decametre amplitude and wavelength (Figs. 5a). Their steeply dipping axial planes are often  
207 gently overturned to the east, and the NNW-trending fold axes plunge gently to the south  
208 (Fig. 5b). The axial plane foliation consists of disjunctive cleavage ranging from fracture to  
209 crenulation cleavage according to lithology. As shown in Figs. 5,  $F_2$  folds are characterised by  
210 extreme variations in shape (open to tight), even within the same lithology, and by axial plane  
211 cleavage generally in the hinge zone of tight folds. On both the eastern and western flanks of  
212 the antiform, where more competent and roughly stratified carbonate formations crop out, the  
213 NNW-trending  $F_2$  folds are open folds of metre to decametre amplitude and wavelength with

214 steeply dipping axial planes. The  $F_2$  folding also affects the marble and calc-silicate hornfels  
215 in the contact aureole of the Gavorrano Granite (Mazzarini *et al.* 2004; Musumeci *et al.*  
216 2005), which is exposed in the antiform hinge zone west and south of Ravi village (Fig. 2). In  
217 this area, the massive hornfels fabric is concentrically folded by  $F_2$  metre-scale upright open  
218 folds that are sometimes gently overturned to the east.

#### 219 *Fault zones*

220 The antiform and associated intrusive rocks are dissected by several fault zones (Figs. 2 and  
221 3) showing reverse-transpressive or normal movements, with normal faulting postdating  
222 reverse faulting (Musumeci *et al.* 2005). The reverse fault zones correspond to the Palaie  
223 Fault and Mt. Calvo Fault on the western flank and the Rigoloccio Fault in the hinge zone.

224 The Palaie Fault is a N-S trending fault zone extending for at least 5 km along the western  
225 flank of the antiform. Fault planes steeply dipping to the east have oblique to down-dip  
226 slickenside striae that indicate a dextral transpressive movement with westward reverse  
227 faulting (Fig. 6a). The latter displacement is dominant in the northern and central portion of  
228 the fault zone. Moreover, southwest of Mt. Calvo, several reverse and/or transpressive metre-  
229 scale fault zones with top-to-the-west movement occur east of the Palaie Fault in the roughly  
230 stratified and/or massive Jurassic carbonate formations of the Tuscan Nappe.

231 The Mt. Calvo Fault, a system of multiple N- to NW-trending reverse faults that dip  
232 gently to moderately to the east, is traceable for for nearly 2 km. Fault planes in the Liassic  
233 carbonate formations cross-cut the bedding which dips moderately to steeply to the west (Fig.  
234 7). Faults correspond to centimetre-thick zones of brittle deformation that affect the rock  
235 extensively, as highlighted by the occurrence of decimetre-spaced fractures parallel to the  
236 fault planes up to several meters away from the faults. Down-dip to slightly oblique  
237 slickenside striae (Figs. 7a and c) highlight the dominant westward reverse movement in this  
238 fault zone (Fig. 6b).

239 The Rigoloccio Fault is a decametre-wide fault zone affecting the intrusive rocks at  
240 the core of the antiform. NW-SE trending fault planes dip moderately to steeply to the NE and  
241 SW. Down-dip to oblique slickenside striae and kinematic indicators reveal top-to-east and  
242 top-to-west reverse movements with dominant top-to-east displacement (Fig. 6c) .  
243 On the eastern flank of the antiform, the Mesozoic carbonate formations are affected by  
244 several reverse faults with down-dip to oblique slickenside striae. In contrast to the western  
245 flank, these fault planes show highly variable orientations ranging from N30E to N150E, and  
246 their distributions do not clearly define fault systems (Fig. 6d).

247 The Caldana-Monticello Fault and Gavorrano Fault are normal faults on the eastern  
248 flank and in the hinge zone of the antiform, respectively. As shown in figures 2 and 3, they  
249 cross-cut the reverse faults and are generally characterised by moderate displacement (100 –  
250 200 m). As documented by Musumeci *et al.* (2005), the Caldana-Monticello Fault is  
251 characterised by transtensive movements with normal faulting in its northern portion, while  
252 the central-southern portion is characterised by transtensive to dextral strike-slip movements.  
253 Inversion of fault slip data for the reverse faults was performed searching for the three  
254 principal stress directions and the stress tensor ratio  $R$  ( $\sigma_2 - \sigma_1 / \sigma_3 - \sigma_1$ ) that best fit the fault-slip  
255 data (Gephart, 1990a, 1990b). Inversion of fault data reveals that reverse faulting is consistent  
256 with a NE – ENE direction of  $\sigma_1$  that ranges from N50°E for the Mt. Calvo Fault to N80°E for  
257 the Palaie Fault (Fig. 6 and Table 1). On the eastern flank of the antiform, although fault  
258 planes have different orientations, the N80°E direction of  $\sigma_1$  (Fig 6d) is consistent with that of  
259 the other fault zones.

260

261 **Discussion**

262 *Gavorrano antiform: evidence of Pliocene shortening*

263 The Gavorrano antiform, although dissected by several fault zones, has an amplitude of at  
264 least 4 km with an along strike length of at least 15 km (Fig. 2). In agreement with Musumeci  
265 *et al.* (2005), it is here interpreted as a thrust ramp fold exploited by the Gavorrano granite  
266 during passive emplacement. Folding resulted from activation of the thrust plane in the  
267 Tuscan Metamorphic Complex and in the evaporitic décollement layer at the base of the  
268 Tuscan Nappe. Deformation and folding of the hornfels fabric indicate that the growth of the  
269 antiform was coeval with granite emplacement (Musumeci *et al.* 2005). On this basis the  
270 antiform formed during the Pliocene, and its development is bracketed between 4.4 Ma and  
271 1.65 Ma. The former is the age of the Gavorrano Granite (Serri *et al.* 1993), the latter the age  
272 of Upper Pliocene-Pleistocene conglomerate deposit containing clasts of granite and Tuscan  
273 Nappe rocks.

274 The mesoscopic structures described above indicate that shortening was achieved through  
275 folding along with reverse and transpressive faulting. The distribution of deformation  
276 structures reveals that folding is the dominant deformation within the well stratified, less  
277 competent formations. Thrusting and reverse faulting is mainly located within the roughly  
278 stratified carbonate formations, as the multiple fault zones on both the eastern and western  
279 flanks indicate (among which the Mt. Calvo reverse fault zone is the best example). The  
280 distribution of folding and faulting structures can be related to the differing competencies of  
281 the Tuscan Nappe formations, with heterogeneous brittle deformation in the lower Mesozoic  
282 carbonate deposits and more homogeneous folding in the upper Mesozoic-Paleogene pelagic  
283 deposits. Likewise, differences in the wavelength and amplitude of F<sub>2</sub> folds suggest poly-  
284 harmonic folding driven by the different competence and thickness of Jurassic and  
285 Cretaceous-Cenozoic formations of the Tuscan Nappe. In this context, the Mt. Calvo and

286 Palaie faults represent two main tectonic structures whose development was mainly  
287 determined by bulk deformation accompanying the growth of the antiform. Indeed both fault  
288 zones can be interpreted as westward backthrust structures characterised by dominant reverse  
289 and transpressive movements. The fact that the Mt. Calvo Fault cross-cuts the westward-  
290 dipping sedimentary bedding in the western flank of the antiform indicates that backthrusting  
291 occurred after nucleation of the antiform and in the late stages of antiform growth. As for the  
292 Palaie Fault, this structure provides clear evidence that westward reverse movements along  
293 steep splay segments were coupled with dextral strike-slip and oblique movements. A  
294 dominant strike-slip movement can account for the juxtaposition along this fault of the  
295 Tuscan Nappe Lower Jurassic formation and the Cretaceous sediments of the Ligurian Unit,  
296 with an apparent vertical displacement of at least 600 – 700 m.

297         The orientation of  $\sigma_1$  (N50°E - N80°E) derived by fault slip data inversion is  
298 consistent with a ENE –WSW shortening direction that is compatible with the NNW-SSE  
299 orientation of  $F_2$  fold axes. The orientation of the stress field and, in particular, the sub-  
300 horizontal attitude of  $\sigma_1$  indicate that granite emplacement did not contribute to the final  
301 structure of the antiform. Indeed, the upright attitude of all  $F_2$  folds and the presence of  
302 backthrust and reverse fault zones and their diffusion throughout the antiform (i.e. not  
303 restricted to the intrusion) clearly indicate that the antiform resulted from regional-scale ENE-  
304 WSW sub-horizontal shortening.

305

#### 306 *Comparison with regional-scale structures*

307 At a regional scale the relevant elements of the Gavorrano antiform are (i) its axial direction,  
308 (ii) the orientation of  $\sigma_1$  and (iii) mesoscopic structures. The NNW strike of the antiform and  
309 related folds and fault zones is parallel to the regional-scale orientation of Neogene tectonic  
310 structures and Upper Miocene-Pleistocene sedimentary basins (Fig. 8). The former are NNW-

311 SSE-trending thrust-related anticlines that deform Upper Miocene-Pliocene deposits. The best  
312 examples are the Mt. Pozzachera anticline (Cerrina Feroni *et al.* 2006) along the Tyrrhenian  
313 coast (Fig. 8), the Mid-Tuscan Ridge Thrust (Fig. 8a) and, farther east, the Cetona Thrust  
314 (Boccaletti & Sani 1998). Sedimentary basins filled by Upper Miocene – Pleistocene deposits  
315 are likewise oriented NNW-SSE. The sedimentary sequences within these basins record  
316 several phases of deformation closed by stratigraphic unconformities that separate deposits of  
317 different ages, with the development of reverse faults and open folds as well as fractures and  
318 joint systems. According to Boccaletti & Sani (1998), deformation in the Neogene –  
319 Quaternary basins of southern Tuscany was linked to four short-lived compressive phases  
320 dated to the (i) Messinian (5.6 Ma), (ii) Early Pliocene (3.8 Ma), (iii) Late Pliocene (2.4 Ma)  
321 and (iv) Middle Pleistocene (0.8 Ma).

322         The Pliocene deformation of sedimentary basins is clearly documented in the Volterra  
323 basin, a wide syncline (Fig. 8) where sediments are affected by NW-trending reverse faults  
324 (Moratti & Bonini 1998). The shortening directions range from NE-SW (Early Pliocene) to E-  
325 W (Late Pliocene). To the south, additional data on Pliocene deformation derive from the  
326 Perolla basin (Fig. 8) some kilometres northeast of the Gavorrano antiform (Moratti & Bonini  
327 1998). In this basin, Upper Messinian and Lower Pliocene conglomerates are deformed by  
328 open folds whose orientation is consistent with a ENE direction of shortening. Moreover, the  
329 Perolla basin corresponds to a NNW- striking open syncline (Fig. 8) in which conjugate joints  
330 and stylolitic pits indicate a NNE shortening direction. In this context, the NE to ENE  
331 shortening direction of the Gavorrano antiform is consistent with the Early Pliocene  
332 deformation recorded in the sedimentary basins (Boccaletti & Sani 1998; Moratti & Bonini  
333 1998).

334         The data reported here relating to the Gavorrano antiform, along with the deformation  
335 recorded in the Upper Miocene – Pleistocene sedimentary basins, indicate that the inner

336 northern Apennines experienced an Early Pliocene phase of crustal shortening. The fact that  
337 the Gavorrano antiform is a thrust ramp fold with the thrust ramp located in the metamorphic  
338 unit below the Tuscan Nappe (Musumeci *et al.* 2005) supports the hypothesis that Neogene  
339 deformation was triggered by the development and/or reactivation of basement thrusts  
340 (Boccaletti & Sani 1998). According to this model, basement thrusting led to the reactivation  
341 of the cover thrust and the development of sedimentary basins in footwall synclines  
342 subsequently deformed during thrust reactivation. The position of the Gavorrano antiform  
343 west of the Mid Tuscan Ridge Thrust (Fig. 8a), i.e. in a more internal position with respect to  
344 the other tectonic structures, suggests the following:

- 345 (i) Pliocene deformation affected the whole Tuscan domain, from the outer portion (Cetona  
346 Thrust; Fig. 8a) to the inner one close to the Tyrrhenian coast;
- 347 (ii) basement-involved thrusting was the main mechanism responsible for deformation of both  
348 tectonic units and Upper Miocene-Pliocene sedimentary basins.
- 349 (iii) basement-involved thrusting led to reactivation of the outer thrusts (Mid Tuscan Ridge  
350 Thrust and Cetona Thrust) as out-of-sequence thrusts. In the inner portion (Tyrrhenian coast),  
351 the development of new thrusts led to the growth of antiformal structures represented best by  
352 the Gavorrano antiform.

353

#### 354 *Shortening vs. extension: implications for the Neogene evolution of the Northern Apennines*

355 The above-documented regime of crustal shortening during the Pliocene argues against the  
356 model of a general extensional regime extending from the northern Tyrrhenian Sea to the  
357 inner northern Apennines (represented by southern Tuscany) for the same period (Carmignani  
358 *et al.* 1994, Decandia *et al.* 1998). Evidence for crustal extension is mainly based on the  
359 occurrence of (i) normal faults within Neogene sedimentary basins and (ii) low- and high-  
360 angle normal faults in the subsurface of the Larderello geothermal field (Brogi *et al.* 2003).

361 Detailed field data reported by Boccaletti *et al.* (1999) reveal that normal faults in the  
362 sedimentary basins cross-cut both the sedimentary sequences and compressive structures.  
363 This means that normal faulting postdates the deposition of sedimentary sequences within the  
364 basins, the development of which is therefore not likely linked to an extensional regime. The  
365 presence of low- and high-angle normal faults in the subsurface of the Larderello geothermal  
366 field was deduced from seismic lines where weak NE-dipping reflections were interpreted as  
367 low-angle normal faults which flatten at a depth of 4 – 5 km corresponding to that of a major  
368 seismic reflector (K-horizon) considered to be a major extensional shear zone (Brogi *et al.*  
369 2003 and references therein). However, the K-horizon, recently renamed H-horizon (Bertini *et*  
370 *al.* 2006), is characterised by a sharp bright spot feature (Gianelli *et al.* 1997) that has been  
371 interpreted as a fluid-saturated zone corresponding to the top of Pliocene intrusions and  
372 related contact aureoles, without any connotation of tectonic structure (Bertini *et al.* 2006).  
373 The low-angle faults imaged by seismic profiles are interpreted as tectonic structures that  
374 developed at the top of structural highs (e.g. the basement anticline in the geothermal field;  
375 Fig. 8) and channel geothermal fluids from depth to the surface (Bertini *et al.* 2006). Since the  
376 low-angle faults sometimes displace the H-horizon, their development postdates the Pliocene  
377 intrusions and can probably be ascribed to Quaternary activity. Likewise, the field expression  
378 of these low-angle faults corresponds to high-angle normal faults that, as reported above, cut  
379 through the sedimentary succession of Pliocene-Pleistocene basins. It therefore follows that  
380 the normal faults reported as evidence of Late Miocene-Pliocene crustal extension in southern  
381 Tuscany correspond to steeply- to low-dipping normal faults of Late Pliocene - Quaternary  
382 age with a maximum vertical throw of some hundred metres. These structures cannot account  
383 for a long-lasting, regional-scale crustal extension and are better attributed to the final growth  
384 and/or collapse of Pliocene compressive structures. This is clearly the case in the Gavorrano



385 antiform, where the development of normal faults on both flanks of the antiform postdates  
386 folding and reverse faulting.

387         In conclusion, the Gavorrano antiform provides clear evidence that during the Pliocene  
388 the inner northern Apennines experienced compressive tectonics which affected both the  
389 nappe stack and the Neogene sedimentary cover. On this basis, the Late Miocene-Pliocene  
390 period in the inner northern Apennines can be regarded as one of crustal shortening rather  
391 than extension. High rock uplift rates ( $> 1.7$  mm/yr) for the Alpi Apuane derived from  
392 thermochronological data (Balestrieri *et al.*, 2003) well fit the proposed Pliocene shortening  
393 phase. According to Molli & Vaselli (2006) and Molli (2007), these data indicate that crustal  
394 shortening continued until the Middle Pliocene by means of out-of-sequence thrusts, leading  
395 to final exhumation of the metamorphic units in the Alpi Apuane.

396         This scenario matches well the hypothesis that since the Late Messinian (6 – 5 Ma) the  
397 degree of subduction rollback and of back-arc extension have decreased in the northern  
398 Tyrrhenian Sea but have increased considerably in the southern Tyrrhenian Sea (Rosenbaum  
399 & Lister 2004). The northern Tyrrhenian Sea-inner northern Apennines cannot therefore be  
400 regarded as a back-arc system. In addition, seismic anisotropy data indicate that only the  
401 southern Tyrrhenian Sea, floored by oceanic crust, represents a true back-arc basin (e.g.  
402 Salimbeni *et al.*, 2007). Although slab roll-back had largely ceased in the Late Miocene (e.g.  
403 Levin *et al.*, 2007), the proposed Pliocene shortening in the inner northern Apennines suggests  
404 that the lower crust could have been the site of crustal attenuation, heat softening and magma  
405 generation, whereas the upper crust continued to behave as a rigid body that sustained most of  
406 the strain arising from the convergence between the Adria and European plates.

407

408 **Conclusions**

409 The Gavorrano antiform formed through Pliocene shortening of the northern Apennine nappe  
410 stack; its development is linked to basement thrusting with associated ramp-thrust folding.  
411 The position of the Gavorrano antiform within the inner domain of the northern Apennines  
412 suggests that the whole sector was affected by crustal shortening during the Pliocene.  
413 Moreover, the occurrence of ramp-thrust folds and the synkinematic emplacement of granites  
414 provides new insight into the tectonic evolution of the inner northern Apennines. These new  
415 data call for a thorough revision of the Neogene tectonic setting of the northern Tyrrhenian  
416 Sea – northern Apennine system, and suggest either the presence of different regimes in the  
417 upper-middle and lower crust or that the northern and southern sectors of the Tyrrhenian sea –  
418 Apennine chain evolved differently.

419

420 **Acknowledgments**

421 The statistical analysis of structural data have been performed by StereoWin 2002 by R.  
422 Allmendinger. Comments of F. Sani, G Molli and G. Corti on the manuscript have been  
423 appreciated. U. Ring and R. Strachan are thanked for constructive review. This research has  
424 been funded by the PRIN-2005 Project “ Integrated geological-geophysical approach for the  
425 study of emplacement modalities and associated structures of magmatic bodies in the upper  
426 crust: the northern Apennines hinterland area” (scientific coordinator F. Sani).

427

428

429

430

431

432 **References**

- 433 ACOCELLA, V. & ROSSETTI, F. 2002. The role of extensional tectonics at different crustal  
434 levels on granite ascent and emplacement: an example from Tuscany (Italy).  
435 *Tectonophysics*, **354**, 71-83.
- 436 BALDI, P., BELLANI, S., CECCARELLI, A., FIOREDELISI, A., SQUARCI, P. & TAFFI, L. 1994.  
437 Correlazioni tra le anomalie termiche ed altri elementi geofisici e strutturali della  
438 Toscana meridionale. *Studi Geologici. Camerti*, **1**, 139 – 149.
- 439 BALESTRIERI, M.L., BERNET, M., BRANDON, M.T., PICOTTI, V., REINERS, P. & ZATTIN, M.  
440 2003. Pliocene and Pleistocene exhumation and uplift of two key areas of the Northern  
441 Apennines. *Quaternari International*, **101-102**, 67 – 73.
- 442 BERTINI, G., CASINI, M., GIANELLI, G. & PANDELI, E. 2006. Geological structures of a long-  
443 living geothermal system, Larderello, Italy. *Terra Nova*, **18**, 163-169.
- 444 BERTINI, G., CAMELI, G.M., COSTANTINI, A., DECANDIA, F.A., DINI, I., ELTER, F.M.,  
445 LAZZAROTTO, A., LIOTTA, D., PANDELI, E. & SANDRELLI, F. 1994. Structural features of  
446 southern Tuscany along the Monti di Campiglia-Rapolano Terme cross-section. *Soc.*  
447 *Geol. Ital. Mem.*, **48**, 51-59.
- 448 BOCCALETTI, M. & SANI, F. 1998. Cover thrust reactivations during Neogene-Quaternary  
449 evolution of the northern Apennines. *Tectonics*, **17**, 112-130.
- 450 BOCCALETTI, M., GIANELLI, G. & SANI, F. 1997. Tectonic regime, granite emplacement and  
451 crustal structure in the inner zone of the Northern Apennines (Tuscany, Italy): a new  
452 hypothesis. *Tectonophysics*, **270**, 127-143.
- 453 BOCCALETTI, M., BONINI, M., MORATTI G. & SANI, F. 1999. Compressive Neogene-  
454 Quaternary tectonics in the hinterland area of the northern Apennines. *Jour. Petroleum*  
455 *Geology*, **22**, 37-60.

456 BOCCALETTI, M., ELTER, P. & GUAZZONE, G. 1971. Plate tectonics model for the development  
457 of the Western Alps and Northern Apennines. *Nature*, **234**, 108-111.

458 BOSSIO, A., COSTANTINI, A., LAZZAROTTO, A., LIOTTA, D., MAZZANTI, R., MAZZEI, R.,  
459 SALVATORINI, G. & SANDRELLI, F. 1993. Rassegna delle conoscenze sulla stratigrafia  
460 del Neoauctono Toscano. *Mem. Soc. Geol. Ital.*, **49**, 17 – 98.

461 BROGI, A., LAZZAROTTO, A., LIOTTA, D. & RANALLI, G. 2003. Extensional shear zones as  
462 imaged by reflection seismic lines: the Larderello geothermal field (central Italy).  
463 *Tectonophysics*, **363**, 127-139.

464 BURGASSI, P.D., DECANDIA, F.A. & LAZZAROTTO, A. 1983. Elementi di stratigrafia e  
465 paleogeografia nelle Colline Metallifere (Toscana) dal Trias al Quaternario. *Mem. Soc.*  
466 *Geol. Ital.*, **25**, 27 – 50.

467 CARELLA, M., FULIGNATI, P., MUSUMECI, G. & SBRANA, A. 2000. Metamorphic consequences  
468 of Neogene thermal anomaly in the northern Apennines (Radicondoli-Travale area,  
469 Larderello geothermal field – Italy). *Geodinamica Acta*, **13**, 345-366.

470 CARMIGNANI, L. & KLIGFIELD, R. 1990. Crustal extension in the Northern Apennines: The  
471 transition from compression to extension in the Alpi Apuane Core Complex. *Tectonics*,  
472 **9**, 1275-1303.

473 CARMIGNANI, L., DECANDIA, F.A., FANTOZZI, P.L., LAZZAROTTO, A., LIOTTA, D. &  
474 MECCHERI, M. 1994. Tertiary extensional tectonics in Tuscany (Northern Apennines,  
475 Italy). *Tectonophysics*, **238**, 295-315.

476 CERRINA FERONI, A., BONINI, M., MARTINELLI, P., MORATTI, G., SANI, F., MONTANARI, D. &  
477 DEL VENTISETTE, C. 2006. Lithological control on thrust-related deformation in the  
478 Sassa-Guardistallo Basin (Northern Apennines hinterland, Italy). *Basin Research*, **18**,  
479 301–321, doi: 10.1111/j.1365-2117.2006.00295.

- 480 DECANDIA, F.A., LAZZAROTTO A., LIOTTA, D., CERNOBORI, L. & NICOLICH, R. 1998. The  
481 CROP 03 traverse: insights on post-collisional evolution of northern Apennines. *Mem.*  
482 *Soc. Geol. It.*, **52**, 427-439.
- 483 DELLA VEDOVA, B., MARSON, I., PANZA, G. F. & SUHADOLC, P. 1991. Upper Mantle  
484 properties of the Tuscan-Tyrrhenian area: A framework for its recent tectonic evolution.  
485 *Tectonophysics*, **195**, 311 – 318.
- 486 DINI A., GIANELLI, G., PUXEDDU, M. & RUGGERI, G. 2005. Origin and evolution of Pliocene–  
487 Pleistocene granites from the Larderello geothermal field (Tuscan Magmatic Province,  
488 Italy). *Lithos*, **81**, 1-31.
- 489 FACCENNA, C., PIROMALLO, C., CRESPO-BLANC, A., JOLIVET, L. & ROSSETTI, F. 2004. Lateral  
490 slab deformation and the origin of the western Mediterranean arcs, *Tectonics*, **23**,  
491 TC1012, doi:10.1029/2002TC001488.
- 492 FINETTI, I.R., BOCCALETTI, M., BONINI, M., DEL BEN, A., GELETTI, R., PIPAN, M. & SANI, F.  
493 2001. Crustal section based on CROP seismic data across North Tyrrhenian–Northern  
494 Apennines-Adriatic Sea. *Tectonophysics*, **343**, 135-163.
- 495 FRANCESCHELLI, M., LEONI, L., MEMMI, I. & PUXEDDU, M. 1986. Regional distribution of Al-  
496 silicates and metamorphic zonation in the low-grade Verrucano metasediments from the  
497 northern Apennines, Italy. *J. Metamorph. Geol.*, **4**, 309 – 321.
- 498 GIANELLI, G., MANZELLA, A. & PUXEDDU, M. 1997. Crustal models of the geothermal areas of  
499 southern Tuscany (Italy). *Tectonophysics*, **281**, 221 – 239.
- 500 GIANNINI, E., LAZZAROTTO, A. & SIGNORINI, R. 1971. Lineamenti di stratigrafia e di tettonica.  
501 In: La Toscana Meridionale, *Rend SIMP*, **27**, 33-168.
- 502 GEPHART, J.W. 1990a. Stress and the direction of slip on fault planes. *Tectonics*, **9**, 845 – 858.

503 GEPHART, J.W. 1990b. FMSI: A FORTRAN program for inverting fault/slickenside and  
504 earthquake focal mechanism data to obtain the regional stress tensor. *Comput. Geosci.*,  
505 **16**, 953 – 989.

506 INNOCENTI, F., ET AL. 1992. Genesis and classification of the rocks of the Tuscan Magmatic  
507 Province: Thirty years after Marinelli's model. *Acta Vulcanol.*, **2**, 247 – 265.

508 JOLIVET, L., ET AL. 1998. Midcrustal shear zones in postorogenic extension: example from the  
509 Tyrrhenian sea. *J. Geophys. Res.*, **103**, 12123-12160.

510 KELLER, J.V.A., MINELLI, G. & PIALLI, G. 1994. Anatomy of late orogenic extension: the  
511 Northern Apennines case. *Tectonophysics*, **238**, 275-294.

512 LEVIN, V., PARK, J., LUCENTE, F.P., MARGHERITI, L. & PONDRELLI, S. 2007. End of subduction  
513 in northern Apennines confirmed by observations of quasi-Loeve waves from the great  
514 2004 Sumatra-Andaman earthquake. *Geophysical Research Letters*, **34**, L04304,  
515 doi:10-1029/2006GL028860.

516 MALINVERNO, A. & RYAN, W.B.F. 1986. Extension on the Tyrrhenian sea and shortening in  
517 the Apennines as result of arc migration driven by sinking of the lithosphere. *Tectonics*,  
518 **5**, 227-245.

519 MAZZARINI, F., CORTI, G., MUSUMECI, G. & INNOCENTI, F. 2004. Tectonic control on laccolith  
520 emplacement in the northern Apennines fold-thrust belt: the Gavorrano intrusion  
521 (southern Tuscany, Italy). In: BREITKREUZ, C. & PETFORD, N. (eds) *Physical geology of*  
522 *high-level magmatic systems*. Geological Society of London, Special Publication, **234**,  
523 151-161.

524 MELETTI, C., PATACCA, E. & SCANDONE, P. 1995. Il sistema di compressione-distensione in  
525 Appennino. In: BORNARD, G., DE VIVO, B., GASPARINI, P. & VALLARIO A., (eds) *50*  
526 *Anni di Attività didattica e Scientifica del Prof. Felice Ippolito*. Liguori, Napoli, pp.  
527 361-370.

- 528 MOLLI, G. 2007. Northern Apennine-Corsica orogenic system: an updated overview. In:  
529 FÜGENSCHUH, B., FROITZHEIM, N. & SIEGISMUND, S. (eds.) "*Tectonics of the Alpine-*  
530 *Carpathian-Dinaride-System*" Geological Society of London, Special Publication, in  
531 press.
- 532 MOLLI, G. & VASELLI, L. 2006. Structures, interference patterns and strain regime during mid-  
533 crustal deformation the Alpi Apuane (Northern Apennines, Italy). In: MAZZOLI, S. &  
534 BUTLER, R. (eds) *Styles of Continental Contraction*. Geological Society of America  
535 Special Paper, 414, 79-93.
- 536 MORATTI, G. & BONINI, M. 1998. Structural development of the Neogene Radicondoli-  
537 Volterra and adjoining hinterland basins in Western Tuscany (Northern Apennines,  
538 Italy). *Geol. J.*, **33**, 223-241.
- 539 MUSUMECI, G., BOCINI, L. & CORSI, R. 2002. Alpine tectonothermal evolution of the Tuscan  
540 Metamorphic Complex in the Larderello geothermal field (northern Apennines, Italy).  
541 *Journal Geological Society London*, **159**, 443-456.
- 542 MUSUMECI, G., MAZZARINI, F., CORTI, G., BARSELLA, M. & MONTANARI, D. 2005. Magma  
543 emplacement in a thrust ramp anticline: The Gavorrano Granite (northern Apennines,  
544 Italy). *Tectonics*, **24**, TC6009, doi:10.1029/2005TC001801, 2005.
- 545 NICOLOSI, I., SPERANZA, F. & CHIAPPINI, M. 2006. Ultrafast oceanic spreading of the Marsili  
546 Basin, southern Tyrrhenian Sea: Evidence from magnetic anomaly analysis. *Geology*,  
547 **34**, 717-720, doi: 10.1130/G22555.1.
- 548 PLATT, J.P. 2007. From orogenic hinterlands to Mediterranean-style back-arc basins: a  
549 comparative analysis. *Journal of the Geological Society, London*, **164**, 297-311,  
550 doi:10.1144/0016-76492006-093.
- 551 PLOMEROVA, J. ET AL. 2006. Seismic anisotropy beneath the northern Apennines (Italy):  
552 Mantle flow or lithosphere fabric? *Earth and Planetary Science Letters*, **247**, 157-170.

553 ROYDEN, L.H., PATACCA, E. & SCANDONE, P. 1987. Segmentation and configuration of  
554 subducted lithosphere in Italy: an important control on thrust belt and foredeep-basin  
555 evolution. *Geology*, **15**, 714-717.

556 ROSENBAUM, G. & LISTER G.S. 2004. Neogene and Quaternary rollback evolution of the  
557 Tyrrhenian Sea, the Apennines, and the Sicilian Maghrebides. *Tectonics*, **23**, TC1013,  
558 doi:10.1029/2003TC001518.

559 SALIMBENI, S., PONDRELLI, S., MARGHERITI, L., LEVIN, V., PARK, J., PLOMEROVA, J. &  
560 BABUSKA, V. 2007. Abrupt change in mantle fabric across northern Apennines detected  
561 using seismic anisotropy. *Geophysical Research Letters*, **34**, L0738,  
562 doi:10.1029/2007gl029302.

563 SAVELLI, C. 2000. Subduction-related episodes of K-alkaline magmatism (15-0.1 Ma) and  
564 geodynamic implications in the north Tyrrhenian – central Italy region: A review. *J.*  
565 *Geodyn.*, **30**, 575-591.

566 SERRI, G., INNOCENTI, F. & MANETTI, P. 1993. Geochemical and petrological evidence of the  
567 subduction of delaminated Adriatic continental lithosphere in the genesis of the  
568 Neogene-Quaternary magmatism of central Italy. *Tectonophysics*, **223**, 117-147.

569 STORTI, F. 1995. Tectonics of Punta Bianca promontory: Insights for the evolution of the  
570 Northern Apennines-Northern Tyrrhenian sea basin. *Tectonics*, **14**, 832-847.

571

572

573

#### 574 **Figure captions**

575 **Fig 1.** Geological sketch map of northern Apennines (modified after Boccaletti & Sani 1998).  
576 Small black box: location of map shown in figure 2; large dashed box: location of the  
577 Larderello geothermal field. AA: Alpi Apuane; CA: Campiglia Antiform; CTA: Cornate –



578 Travale Antiform; GA: Gavorrano Antiform; LGF: Larderello geothermal field; MP: Monti  
579 Pisani; MTR: Mid Tuscan Ridge; MA: Monte Argentario promontory.

580

581 **Fig 2.** Geological sketch map of Gavorrano structure (modified after Musumeci *et al.*, 2005).

582 LU: Ligurian Unit; TN: Tuscan Nappe; TMC: Tuscan Metamorphic Complex; CMF:  
583 Caldana-Monticello Fault; GF: Gavorrano Fault; MCF: Monte Calvo Fault; PF: Palaie Fault;  
584 RF: Rigoloccio Fault.

585

586 **Fig. 3.** Geological cross section of Gavorrano structure (modified after Musumeci *et al.*,  
587 2005). CMF: Caldana-Monticello Fault; GF: Gavorrano Fault; MCF: Monte Calvo Fault; PF:  
588 Palaie Fault; RF: Rigoloccio Fault.

589

590 **Fig 4.** Lower emisphere, equal area projection stereogram of  $S_0$  foliation poles contours.  
591 Black circle: calculated  $F_2$  axis.

592

593 **Fig 5.** (a) Hand drawing of mesoscopic  $F_2$  folds on Diaspri Fm.. (b) Lower emisphere equal  
594 area projection stereogram of  $S_0$  foliation poles contours. Black circle: calculated  $F_2$  axis,  
595 empty circles: measured  $F_2$  axes.

596

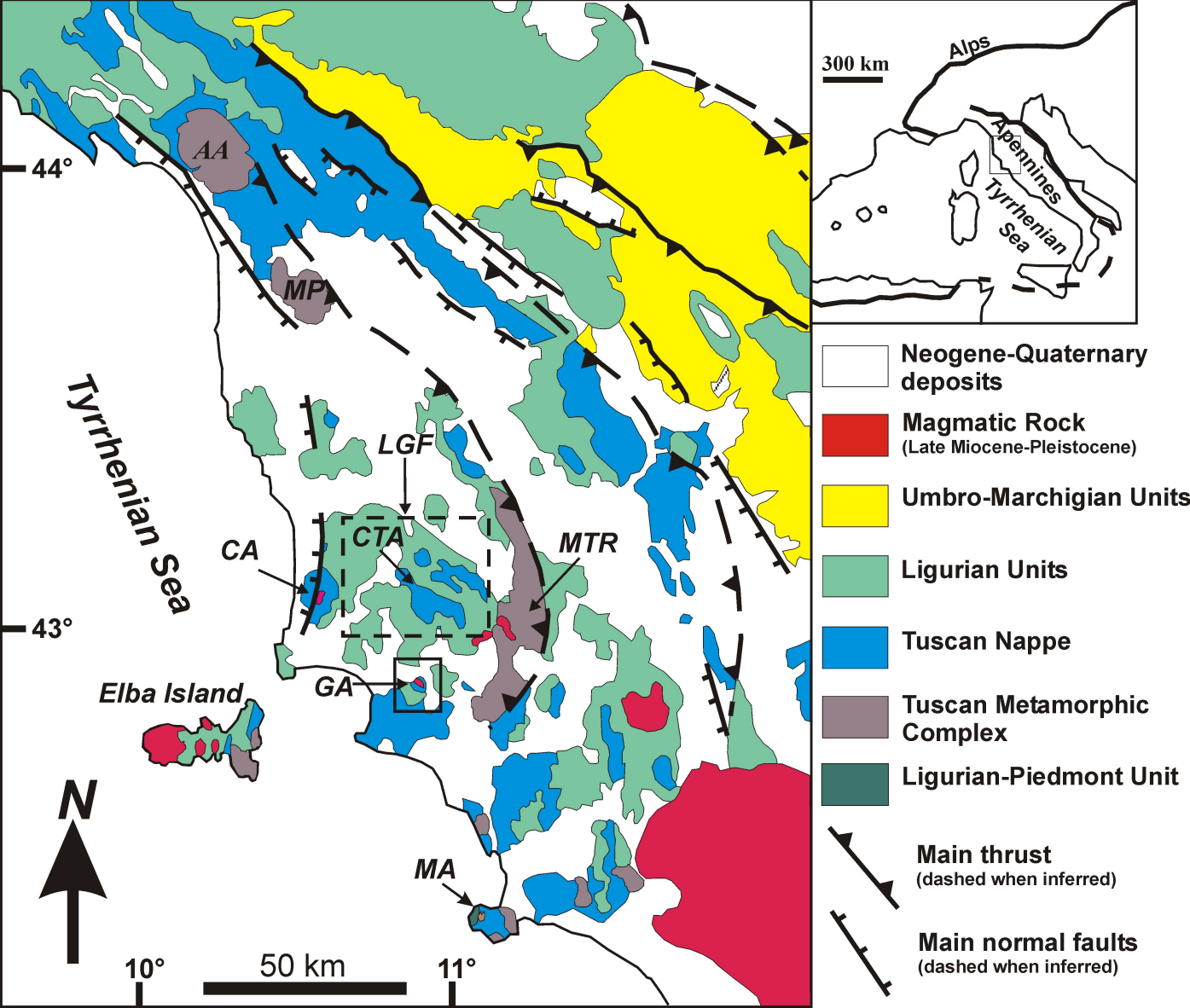
597 **Fig 6.** Tectonic sketch map of Gavorrano antiform and stereograms (lower emisphere, equal  
598 area projection) of structural elements and slip data in fault zones. (a) Palaie Fault. (b) Mt  
599 Calvo Fault. (c) Rigoloccio Fault. (d) Eastern flank faults. Fault symbols, great circle: fault  
600 planes, small black circle: slickenside striae. Slip data symbols, black triangle:  $\sigma_1$ ; black  
601 square:  $\sigma_2$ ; black circle:  $\sigma_3$ . LU: Ligurian Unit; TN: Tuscan Nappe; TMC: Tuscan  
602 Metamorphic Complex; MCF: Monte Calvo Fault; PF: Palaie Fault; RF: Rigoloccio Fault.

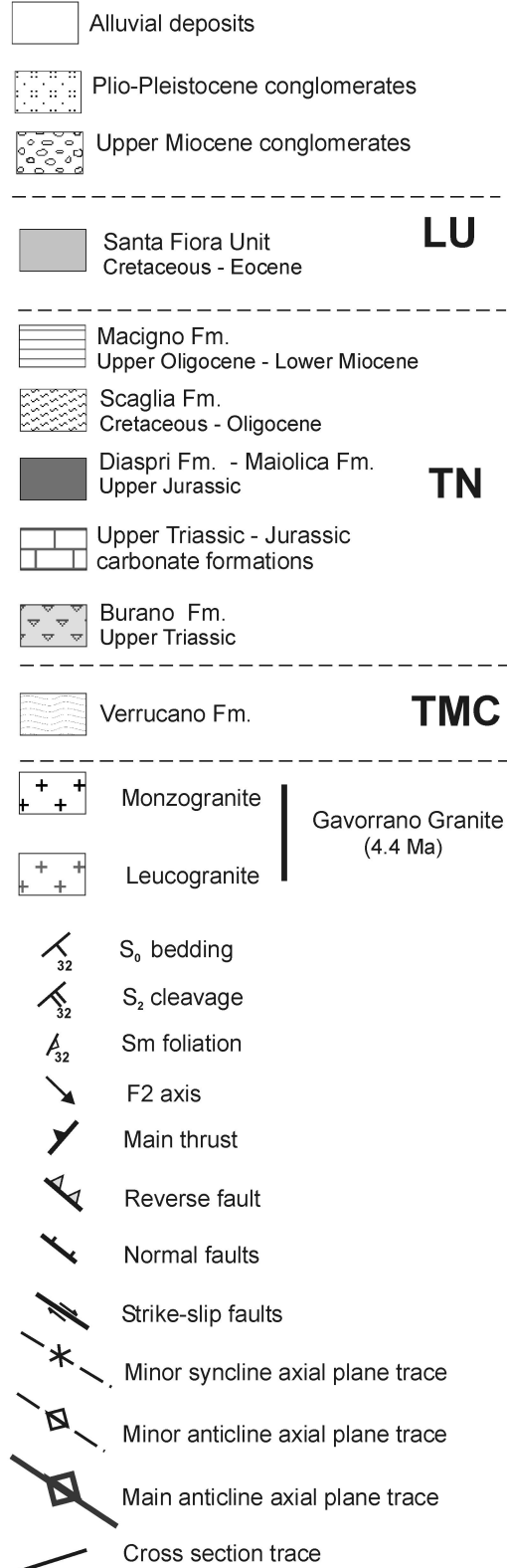
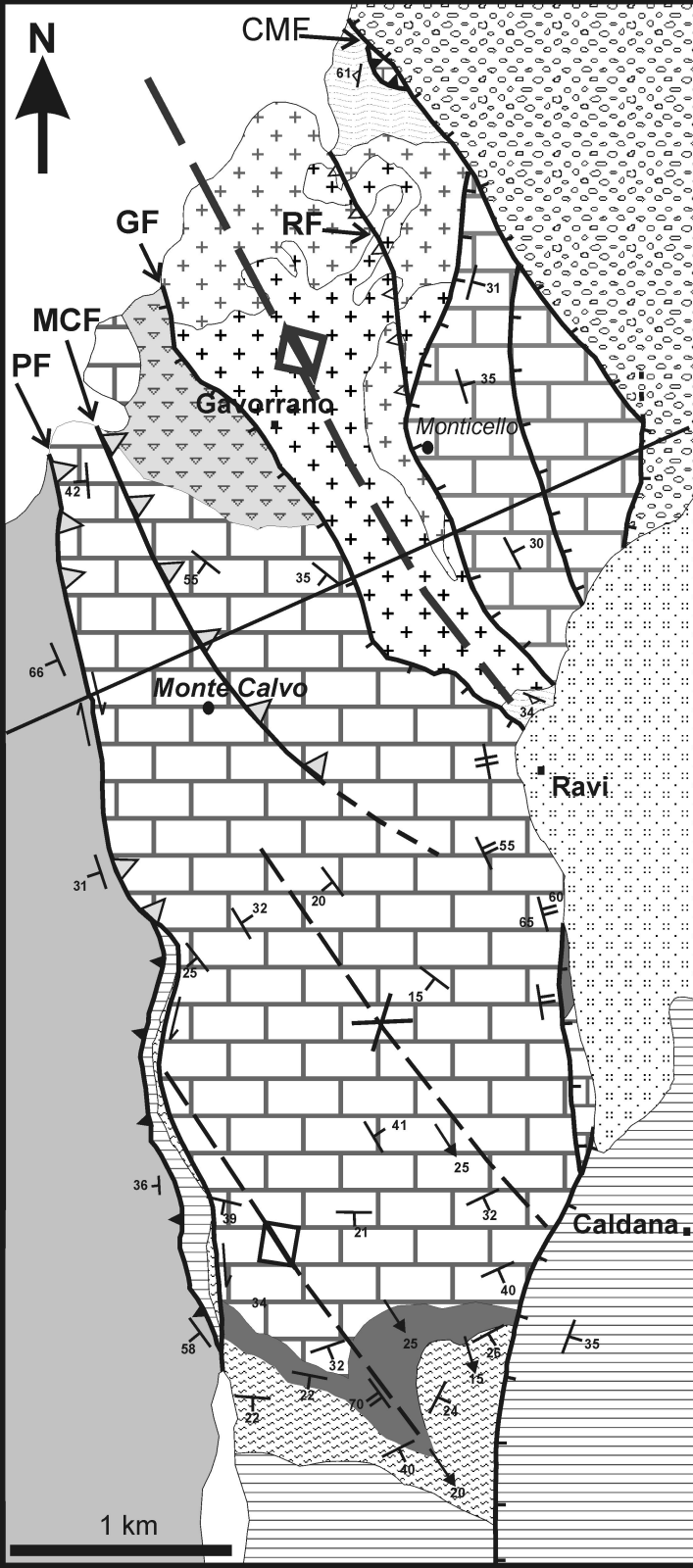
603

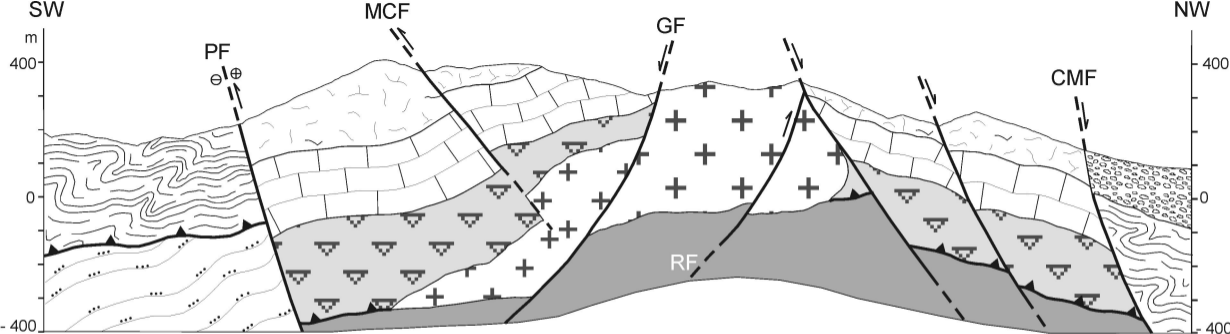
604 **Fig. 7.** Field photo of Mt Calvo Fault. **(a)** Reverse fault plane moderately dipping toward east  
605 with down-dip slickenside striae (dashed white arrow) and top to the west displacement (half  
606 white arrow), scale bar 1,5 m. **(b)** West dipping sedimentary bedding cross-cut by east  
607 dipping reverse fault (dashed white line) with top to the west displacement (half black arrow),  
608 scale bar 2 m. **(c)** Lower hemisphere equal area projection stereogram of Mt. Calvo Fault.  
609 Filled circle: poles of sedimentary bedding; filled triangle: poles of fault planes; empty  
610 triangle: pole of fractures associated to the fault planes.

611

612 **Fig. 8.** Geological-structural sketch map of southern Tuscany (modified after Moratti &  
613 Bonini 1998) showing position of main anticline and syncline deforming Neogene basins and  
614 location of basement anticline structures. Box numbers are referred to the following structures  
615 1: Gavorrano antiform; 2: Campiglia antiform; 3: Mt. Pozzacchera anticline; 4: Larderello  
616 anticline, 5: Scarpenata anticline; 6: S. Maria backthrust; 7: Fine syncline; 8: Volterra  
617 syncline; 9: Scarpenata syncline; 10: Perolla syncline; 11: Sassa syncline. In the inset **(a)** are  
618 reported the position of the northern Apennines main thrust systems : MTRT: Mid Tuscan  
619 Ridge Thrust, CT: Cetona Thrust, CFT: Cervarola Falterona Thrust, PAT: Padan Adriatic  
620 Thrust.







Upper  
Miocene  
Conglomerates

Ligurian  
Units

Macigno  
Fm.

Calcare  
Massiccio Fm.

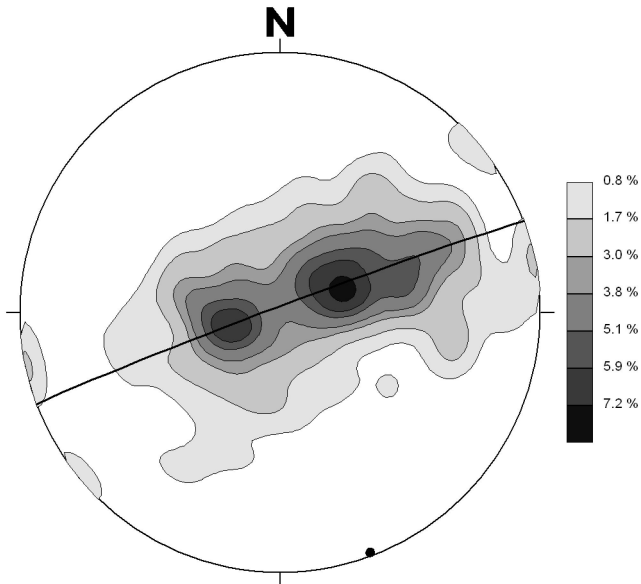
Calcare e marna  
a Rhaetavicola Fm.

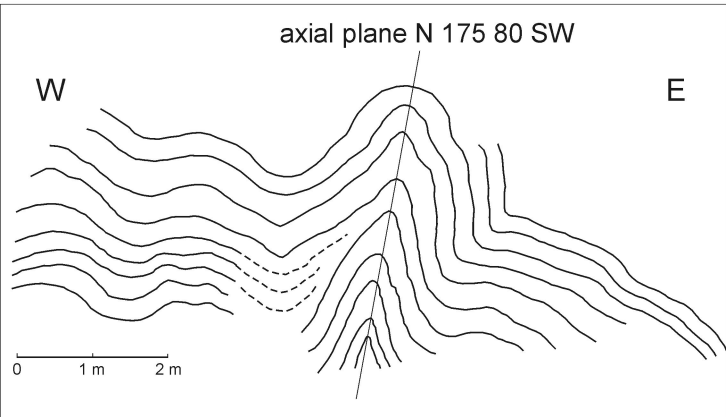
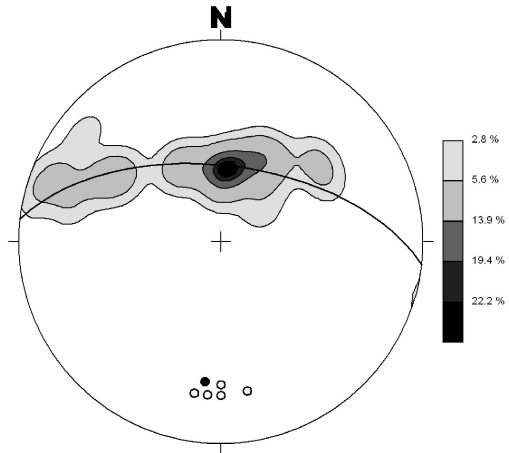
Calcare  
Cavernoso Fm.

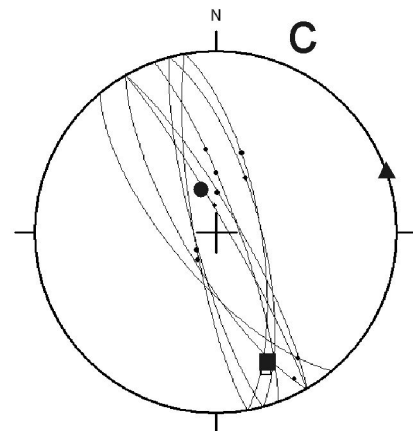
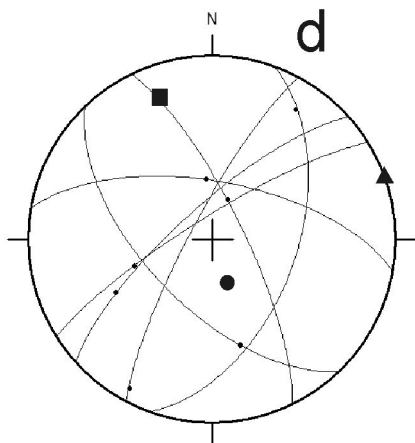
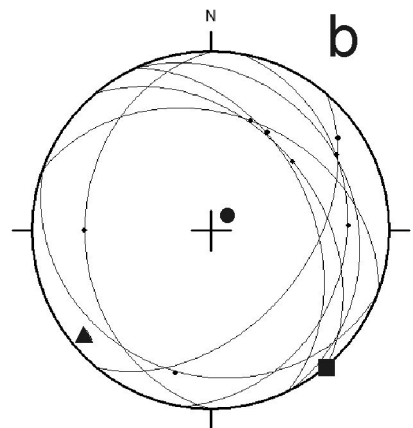
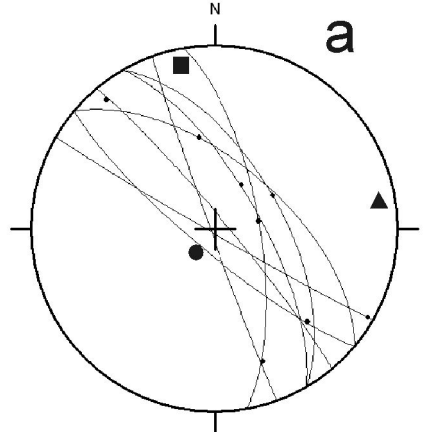
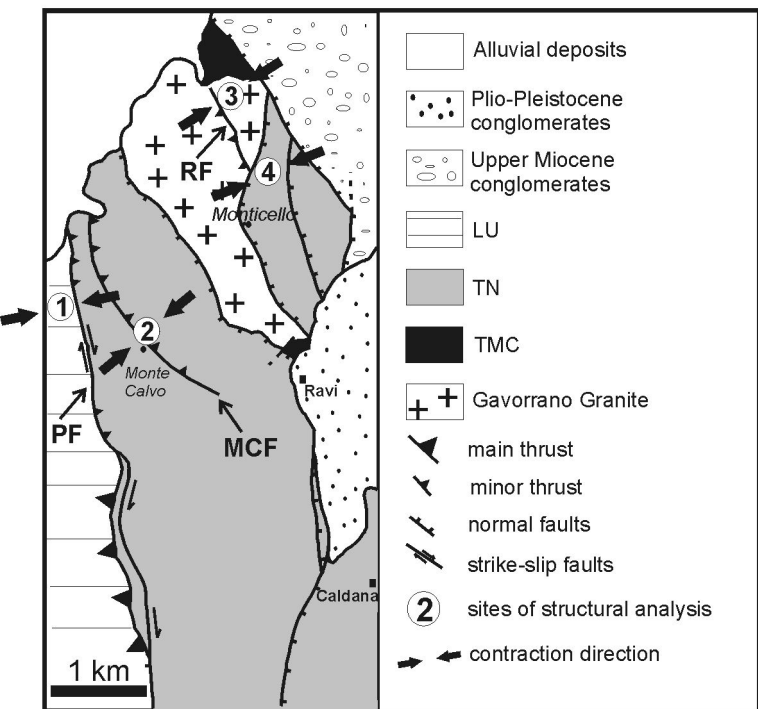
Gavorrano  
Granite

Verrucano  
Fm.

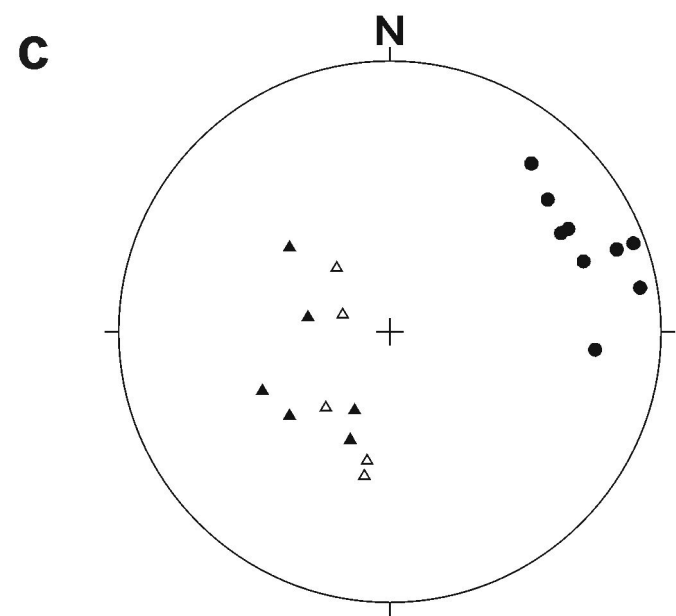
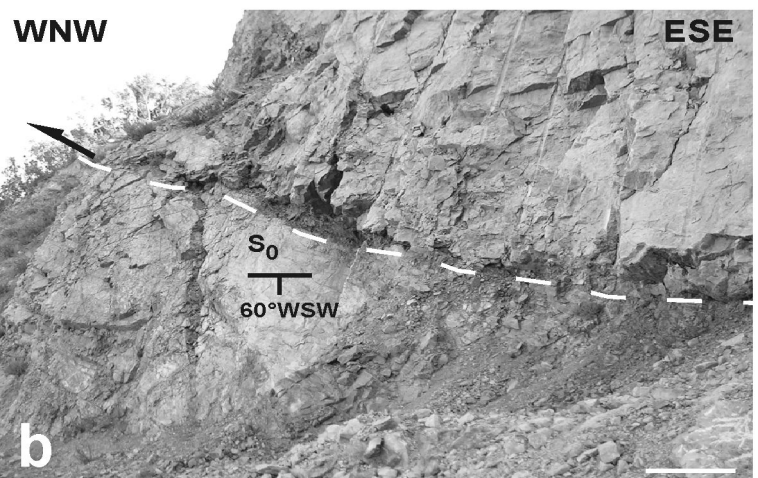
Thrust  
Faults



**a****b**







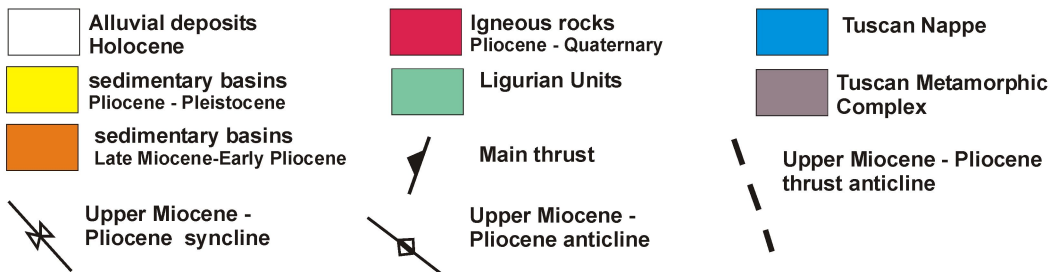
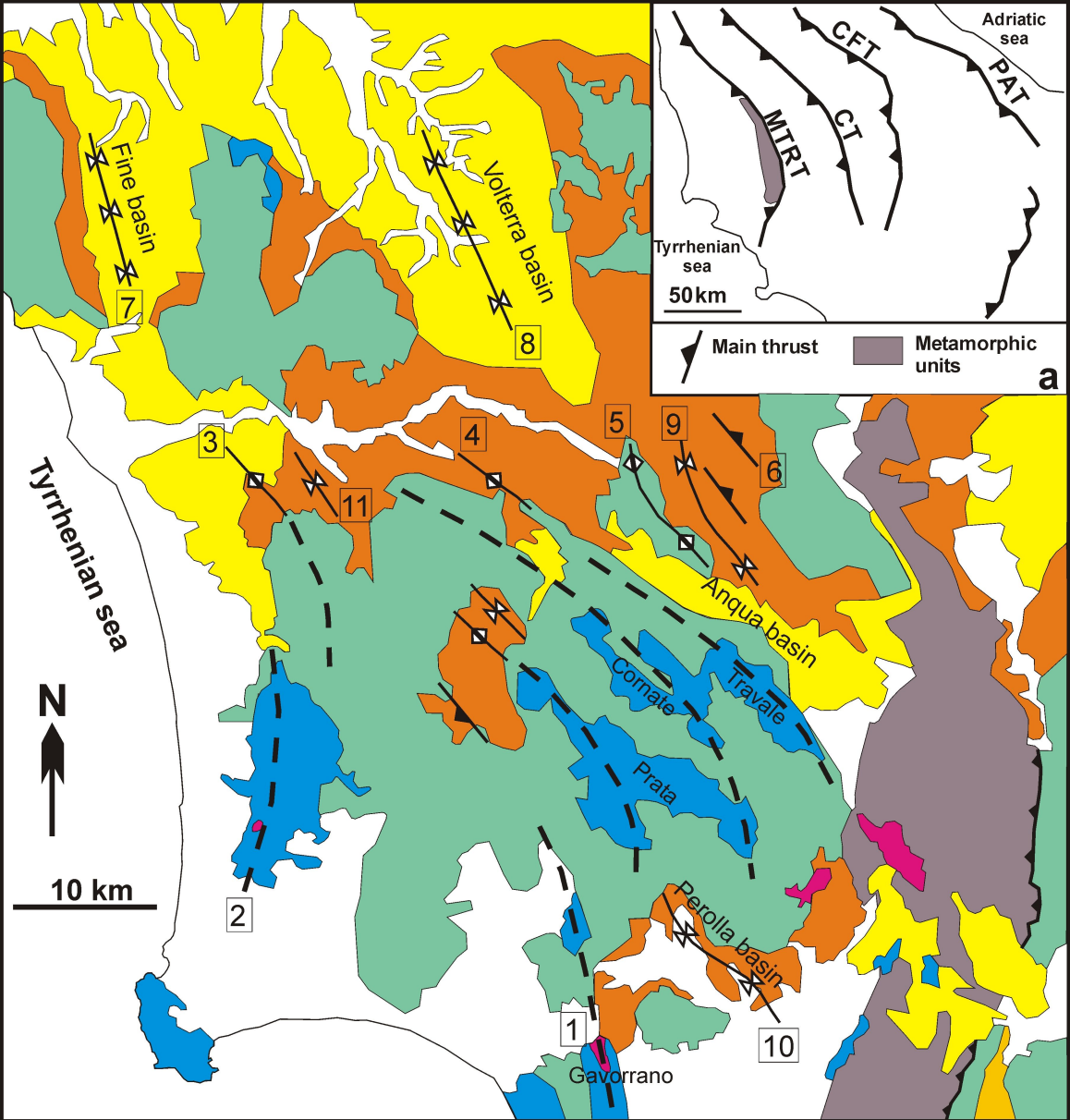


**Table 1.** *Inversion of fault-slip data in the Gavorrano antiform*

site	fault	movement	<i>trend°/plunge°</i>			Tensor Fit (%)	Ratio Tensor Shape	n faults
			$\sigma_1$	$\sigma_2$	$\sigma_3$			
1	Palaie	drs	80°/10°	348°/9°	214°/75°	85.9	0.50	8
2	Monte Calvo	r	230°/10°	140°/0°	50°/80°	87.8	0.68	8
3	Rigoloccio	r	70°/0°	160°/20°	340°/70°	76.2	0.75	10
4	Gavorrano East	-	70°/0°	340°/20°	160°/70°	57.3	0.89	7

r: reverse movement; drs: dextral oblique reverse movement; - not defined